Int. J. Radiation Oncology Biol. Phys., Vol. 79, No. 1, pp. 247–254, 2011

0360-3016/$–see front matter

ELSEVIER

doi:10.1016/j.ijrobp.2010.07.022

BIOLOGY CONTRIBUTION

DYNAMICS OF DELAYED *P53* MUTATIONS IN MICE GIVEN WHOLE-BODY IRRADIATION AT 8 WEEKS

Ryuji Okazaki, M.D., Ph.D.,* Akira Ootsuyama, D.V.M., Ph.D.,* Hiroyo Kakihara, BS,* Yo Mabuchi, Ph.D.,† Yumi Matsuzaki, M.D., Ph.D.,† Yuichi Michikawa, Ph.D.,‡ Takashi Imai, Ph.D.,‡ and Toshiyuki Norimura, Ph.D.*

*Department of Radiation Biology and Health, School of Medicine, University of Occupational and Environmental Health, Japan, Kitakyushu, Japan; †Department of Physiology, Keio University, School of Medicine, Tokyo, Japan; and ‡RadGenomics Project, Research Center for Charged Particle Therapy, National Institute of Radiological Sciences, Chiba, Japan

Purpose: Ionizing irradiation might induce delayed genotoxic effects in a p53-dependent manner. However, a few reports have shown a *p53* mutation as a delayed effect of radiation. In this study, we investigated the *p53* gene mutation by the translocation frequency in chromosome 11, loss of *p53* alleles, *p53* gene methylation, *p53* nucleotide sequence, and p53 protein expression/phosphorylation in $p53^{+/+}$ and $p53^{+/-}$ mice after irradiation at a young age.
Methods and Materials: $p53^{+/+}$ and $p53^{+/-}$ mice were exposed to 3 Gy of whole-body irradiation at 8 weeks of age. Chromosome instability was evaluated by fluorescence *in situ* hybridization analysis. *p53* allele loss was evaluated by polymerase chain reaction, and *p53* methylation was evaluated by methylation-specific polymerase chain reaction. *p53* sequence analysis was performed. p53 protein expression was evaluated by Western blotting.
Results: The translocation frequency in chromosome 11 showed a delayed increase after irradiation. In old irradiated mice, the number of mice that showed *p53* allele loss and *p53* methylation increased compared to these numbers in old non-irradiated mice. In two old irradiated $p53^{+/-}$ mice, the *p53* sequence showed heteromutation. In old irradiated mice, the p53 and phospho-p53 protein expressions decreased compared to old non-irradiated mice.
Conclusion: We concluded that irradiation at a young age induced delayed *p53* mutations and p53 protein suppression. © 2011 Elsevier Inc.

Irradiation, Mouse, p53, Delayed mutation, Genomic instability.

INTRODUCTION

The induction of delayed effects by ionizing radiation has been reported as delayed mutation (1), delayed reproductive cell death (2), increased late mortality rate (3), and delayed chromosomal aberrations (4, 5). An early report of a delayed effect of radiation was that chromosomal instability increased in skin fibroblasts from mouse fetuses after zygote X-irradiation (4). Also, radiation-induced chromosomal instability was reported in X-irradiated primary human lymphocytes (5). The radiation-induced increase in genomic instability is apparently a general phenomenon (6). Genomic instability apparently promotes cancer development (7, 8). Atomic bomb survivors who were exposed to whole-body radiation had increases in a wide range of malignancies (3, 7). In the Chernobyl accident, people who were exposed to radioactive isotopes had increased thyroid carcinoma and breast cancer (8).

p53 is one of the important genes that are related to genomic instability (9). In *p53*-defective cells, heat shock factor 1-mediated aneuploidy was more common (10). With the disruption of both Chk2 and p53 function after irradiation-induced DNA damage, a synergistic increase in genomic instability was seen in an *in vitro* study (11). In *p53* ser 23 mutant mice, lymphoma and sarcoma developed, whereas alternatively, in a p53-stabilized status, proper apoptosis function was maintained and mice were protected from tumorigenesis (12). In precancerous lesions, wild-type p53 function is retained. When the p53 function is lost, the precancerous lesion can become cancerous (9). However, it is not clear how radiation induces *p53* gene mutation.

Reprint requests to: Ryuji Okazaki, M.D., Ph.D., Department of Radiation Biology and Health, School of Medicine, University of Occupational and Environmental Health, Japan, 1-1 Iseigaoka Yahatanishi-ku, Kitakyushu, 807-8555, Japan. Tel: (+81) 0-93-603-1611, ext. 4635; Fax: (+81) 0-93-692-0559; E-mail: ryuji-o@med.uoeh-u.ac.jp

Supported in part by UOEH grant for Advanced Research (H18-3), UOEH Research Grant for Promotion of Occupational Health from University of Occupational and Environmental Health (No. 909) and Grants-in-Aid for Scientific Research (C) from Japan Society for the Promotion of Science (No. 19510061).

Conflict of interest: none.

Acknowledgment—The authors thank Mr. Sadafumi Suzuki of Keio University for technical assistance.

Received March 16, 2010, and in revised form July 5, 2010. Accepted for publication July 7, 2010.

In a previous study, we showed that X-irradiation at a young age induces delayed T-cell receptor (TCR) mutations (13). In other words, $CD3^-CD4^+$ T-cell fraction was increased at old age after irradiation at a young age. In $p53^{+/+}$ mice at 72 weeks of age after irradiation at 8 weeks of age, the TCR variant fraction ($CD3^-CD4^+$ cells / $CD3^+CD4^+$ cells) was 30.2×10^{-4}; alternatively, the TCR variant fraction was 7.1×10^{-4} in the control group. Inasmuch as delayed TCR mutation in $p53^{+/-}$ mice appeared earlier than that in $p53^{+/+}$ mice, we speculated that the delayed mutation induced by irradiation might be p53 dependent. In this study, to clarify the effect of irradiation at a young age on the *p53* gene, we evaluated the translocation frequency in chromosome 11, on which the mouse *p53* locus is found (14); loss of *p53* alleles; *p53* methylation; *p53* sequence; and p53 protein expression in $p53^{+/+}$ and $p53^{+/-}$ mice after 3 Gy irradiation at 8 weeks of age. We observed delayed *p53* disorders and p53 protein suppression after irradiation at a young age.

METHODS AND MATERIALS

Experimental animals

Mice carrying a disrupted, nonfunctional *p53* gene ($p53^{-/-}$) were derived by homologous recombination in an embryonic stem cell line from 129/SvJ mice as previously described (15). Wild-type mice of the parental inbred strain were used as controls for $p53^{+/+}$ mice. $p53^{+/-}$ mice were obtained by crossing male $p53^{-/-}$ mice with female $p53^{+/+}$ mice. The experimental protocols were approved by the Ethics Review Committee for Animal Experimentation of the University of Occupational and Environmental Health, Japan, Kitakyushu, Japan.

Radiation treatments

$p53^{+/+}$ and $p53^{+/-}$ mice were randomly divided into an irradiated group or a nonirradiated group at 8 weeks of age. The irradiated groups were given a whole-body dose of 3 Gy (0.82 Gy/min) at 8 weeks of age from a ^{137}Cs Gammacell 40 Exactor (MDS Nordion, Canada), and the nonirradiated groups were sham irradiated.

Cell treatment and fluorescence in situ hybridization

Splenocytes were plated in six-well plates at 2×10^5 cells/well and were maintained in RPMI-1640 (Gibco's 31800) (Invitrogen, Carlsbad, CA) supplemented with 15% fetal bovine serum, 300 mg/mL Concanavalin A, and 5 mM mercaptoethanol. After growth for 62 to 72 hours, 0.02 mg/mL colcemid was added and incubated for 30 minutes. After centrifuging at 1,000 rpm, cells were treated with 0.075 M KCl at room temperature for 20 minutes. After again centrifuging at 1,000 rpm, cells were fixed by Carnoi solution (methanol:acetic acid = 3:1 v/v) for 5 minutes. After centrifuging at 1,200 rpm, the supernatant was discarded, and Carnoi solution was added. The sample was centrifuged at 1,200 rpm again, and the cell pellet was put on a glass slide and dried at 37°C.

To identify translocations on chromosome 11 of splenocytes, fluorescence *in situ* hybridization (FISH) analysis was performed using the procedures recommended by the manufacturer (CamBio Ltd., Cambridge, UK). Chromosomes were washed by ×0.4 and ×2 SSC in 0.05% Tween 20 at 70°C for 2 minutes each, and then the samples were treated with rabbit anti-FITC (fluorescein isothiocyanate) and FITC goat anti-rabbit IgG using a Dual Color Kit (CamBio) according to the manufacturer's instructions. Finally, the chromosomes were counterstained with DAPI (4',6-diamidino-2-phenylindole).

Sorting into $CD3^-CD4^+$ cells and $CD3^+CD4^+$ cells from splenocytes

T cells from spleens were enriched by the nylon-wool-column method, as described previously (13), and 500,000 T cells were stained with PE-anti CD4 and FITC-anti CD3 antibodies (Pharmingen, San Diego, CA) on ice for 30 minutes. After antibody staining, the cells were washed with an excess amount of HBSS+ and resuspended at 1×10^7 cells/mL in HBSS+ containing 2 μg/mL propidium iodide (Sigma Chemical Co., St. Louis, MO, USA). Cells were sorted into $CD3^-CD4^+$ cells and $CD3^+CD4^+$ cells by Moflo (Beckman Coulter, Brea, CA, USA), and the data were analyzed using Flowjo software (Tomy Digital Biology Co., Ltd., Tokyo, Japan).

Preparation of genomic DNA

Genomic DNA from $CD3^+CD4^+$ cells was isolated using the QuickGene DNA (Fujifilm Holdings Corporation, Tokyo, Japan) whole blood kit according to the manufacturer's instructions. Genomic DNA of $CD3^-CD4^+$ cells was prepared directly by the igMDA (in-gel multiple displacement amplification) method, as described previously (16).

Determination of p53 allele loss, wild-type p53/p53-pseudogene ratio

For the determination of the loss of *p53* alleles, we used the wild-type *p53*/*p53*-pseudogene ratio according to the method of Hulla *et al*. (17).

Bisulfite conversion and methylation-specific polymerase chain reaction

Approximately 1 μg of DNA from $CD3^+CD4^+$ cells was treated with sodium bisulfite using the EpiTect Bisulfite kit (Qiagen, Hilden, Germany) according to the manufacturer's instructions.

CpG islands in the *p53* gene were searched and polymerase chain reaction (PCR) primer sets were designed by Methyl Primer Express Software v1.0 (Applied Biosystems, Inc., Foster City, CA). PCR

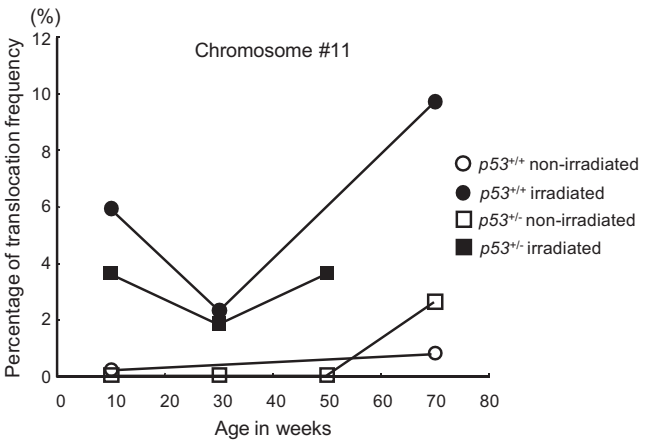

Fig. 1. Time course of the translocation frequency in chromosome 11 in $p53^{+/+}$ and $p53^{+/-}$ mice after 3 Gy whole-body irradiation at 8 weeks of age. Fluorescence *in situ* hybridization analysis was performed. There were at least three mice in each group. As for the translocation frequency of chromosome 11 in each group, the total abnormal cell number was divided by the total cell number.

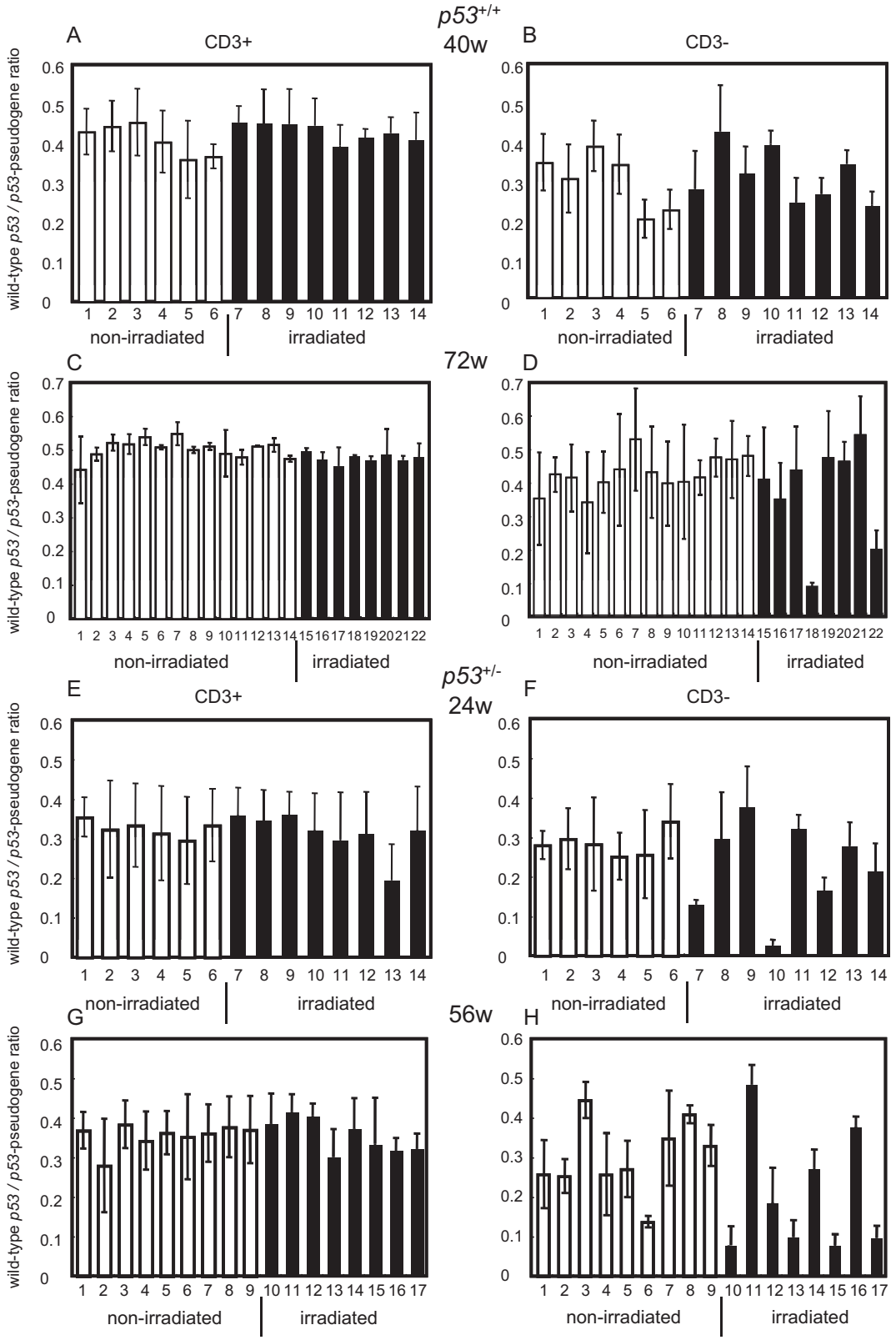

Fig. 2. Time course of the *p53* allele loss in $p53^{+/+}$ and $p53^{+/-}$ mice after 3 Gy whole-body irradiation at 8 weeks of age. (A, B) $p53^{+/+}$ mice at 40 weeks of age. The number on the X-axis shows the same mouse. (C, D) $p53^{+/+}$ mice at 72 weeks of age. The number on the X-axis shows the same mouse. (E, F) $p53^{+/-}$ mice at 24 weeks of age. The number on the X-axis shows the same mouse. (G, H) $p53^{+/-}$ mice at 56 weeks of age. The number on the X-axis shows the same mouse. (A, C, E, G) $CD3^{+}CD4^{+}$ cells. (B, D, F, H) $CD3^{-}CD4^{+}$ cells. The wild-type *p53*/*p53*-pseudogene ratio was calculated as wild-type *p53*/(wild-type *p53* + *p53*-pseudogene). At least three independent experiments were performed for each sample. Data are presented as means ± standard deviation.

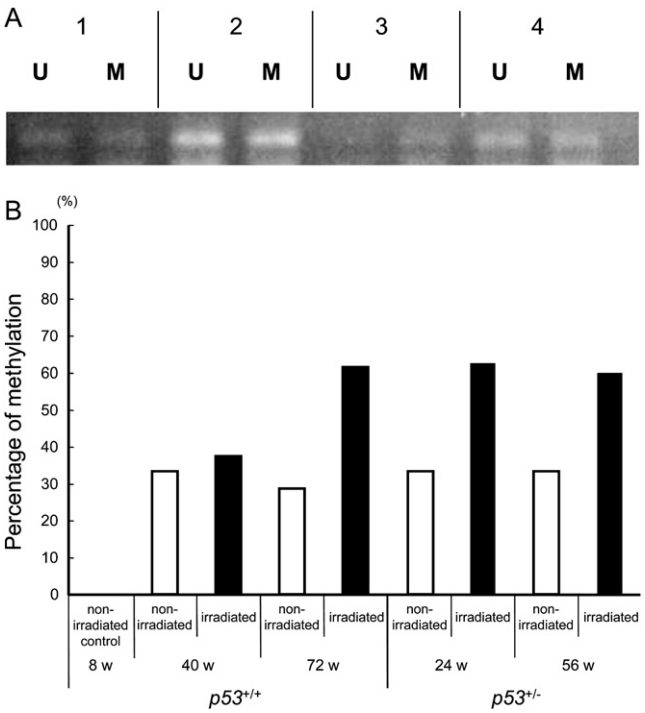

Fig. 3. MSP (methylation specific PCR) assay for *p53* in $CD3^+CD4^+$ cells in $p53^{+/+}$ and $p53^{+/-}$ mice after 3 Gy whole-body irradiation at 8 weeks of age. (A) Bisulfite-treated DNA was amplified with primers specific for either an unmethylated (U) or a methylated (M) *p53*. Lane 1, 2: nonirradiated; Lane 3, 4: irradiated. Representative data are shown. (B) Time course of percentage of the *p53* methylation. Each group contained 5 to 13 mice.

primer sets for *p53*-UnMethylation were sense 5'- ATC GTT ATT CGG TTT GTT TTC -3' and antisense 5'- CGA ACA CGA CTC CCA ACT AA, and those for *p53*-Metylation were sense 5'- ATC GTT ATT CGG TTT GTT TTC -3' and antisense 5'- CGA ACA CGA CTC CCA GCT AA-3'. PCR amplification was performed using the EpiTect MSP kit (Qiagen). Thermal cycling conditions were as follows: one cycle at 95°C for 10 minutes; 30 cycles at 94°C for 15 seconds, 55°C for 30 seconds, and 72°C for 30 seconds; and one cycle at 72°C for 10 minutes.

PCR amplification and sequence analysis

The PCR amplification was performed using gene-specific PCR primers and TaKaRa Ex Taq Hot Start Version (Takara Bio Inc., Otsu, Shiga, Japan) and was allowed to proceed in a TaKaRa PCR thermal cycler (Takara Bio Inc.). PCR primer sets for exon 7 of *p53* were sense 5'-TTA ACA GCA GTC TCT GGG AGA AG-3' and antisense 5'-GTT TCT GTT CCA CGA GTC CC-3'. Thermal cycling conditions were as follows: one cycle at 95°C for 3 minutes; 30 cycles at 95°C for 30 seconds, 63°C for 45 seconds, and 72°C for 1 minute; and one cycle at 72°C for 5 minutes.

Because the number of $CD3^-CD4^+$ cells was small, 1 mL of the cell suspension (from 100 to 1,000 cells) was incubated with 5 mL of 10x Ex Taq buffer in a TaKaRa Ex Taq Hot Start Version (Takara Bio Inc.), 1 mL of each of the primers and 37.75 mL of distilled water at 98°C for 5 minutes before PCR thermal cycling. Then, 4 mL of dNTP and 0.25 ml of Taq were added, and the thermal cycle was simultaneously started. Thermal cycling conditions were as follows: 30 cycles at 95°C for 30 seconds, 63°C for 45 seconds, and 72°C for 1 minute; and one cycle at 72°C for 5 minutes.

The DNA sequencing was performed using the BigDye terminator v3.1 cycle sequencing kit (Applied Biosystems) according to the manufacturer's instructions. PCR primer sets for exon 7 of *p53* were sense 5'-CAG GTG GAA TAT CCC TAC TCT ACA A -3'and antisense 5'-GTT TCT GTT CCA CGA GTC CC-3'. Finally, the DNA sequencing reactions were purified using a BigDye XTerminater purification kit (Applied Biosystems) according to the manufacturer's instructions. The DNA sequencing reactions were run on a 3130/3130xl genetic analyzer (Applied Biosystems). The sequencing was analyzed by a sequencing analysis software (Applied Biosystems).

Western blot analysis

Western blotting protocol followed a NuPage Western blotting system (Invitrogen, Carlsbad, CA) as described previously (18). Ten milligrams of protein from mouse spleen were used. The first antibodies were anti-p53 antibody (BD biosciences, San Jose, CA) and anti-phospho-p53 (ser15/18) (Calbiochem, San Diego, CA) anti-actin (Santa Cruz Biotechnology) (1:1,000 dilution in 1% skimmed milk in TBS-T).

Statistical analysis

In the Western blot assay, the expression levels of p53 and phospho-p53 were normalized to actin, and then Student's *t* test was used to determine the difference between irradiated mice and nonirradiated mice at each time point. A *p* value less than 0.05 was considered to be significant.

RESULTS

Time course of translocation frequency in chromosome 11 in $p53^{+/+}$ and $p53^{+/-}$ mice after 3 Gy whole-body irradiation at 8 weeks of age

The FISH data show a similar time course of the translocation frequency in chromosome 11 in $p53^{+/+}$ and $p53^{+/-}$ mice after irradiation at 8 weeks of age (Fig. 1). In the irradiated mice, the translocation frequency was at the maximum level at 10 weeks of age and then decreased at 24 weeks of age. In $p53^{+/+}$ mice and $p53^{+/-}$ mice, the translocation frequency in the irradiated mice increased again compared to that in the non-irradiated mice at 72 weeks of age and at 40 weeks of age, respectively. In non-irradiated $p53^{+/-}$ mice, the translocation frequency increased at 72 weeks of age.

Time course of p53 allele loss in $p53^{+/+}$ and $p53^{+/-}$ mice after 3 Gy whole-body irradiation at 8 weeks of age

In the $CD3^+CD4^+$ cells of all mice, there were no significant differences in *p53* allele loss between the irradiated and non-irradiated mice (Fig. 2A, C, E, G).

In the $CD3^-CD4^+$ cells in $p53^{+/+}$ mice at 40 weeks of age, there were no remarkable differences in *p53* allele loss between the irradiated and non-irradiated mice (Fig. 2B). In the $CD3^-CD4^+$ cells in the irradiated $p53^{+/+}$ mice at 72 weeks of age, two of the eight mice showed *p53* allele loss (Fig. 2D). In the $CD3^-CD4^+$ cells in the irradiated $p53^{+/-}$ mice at 24 weeks of age, three of the eight mice showed *p53* allele loss (Fig. 2F). In the $CD3^-CD4^+$ cells in the irradiated $p53^{+/-}$ mice at 56 weeks of age, four of the eight mice showed *p53* allele loss (Fig. 2H). Last, in the $CD3^-CD4^+$ cells in the

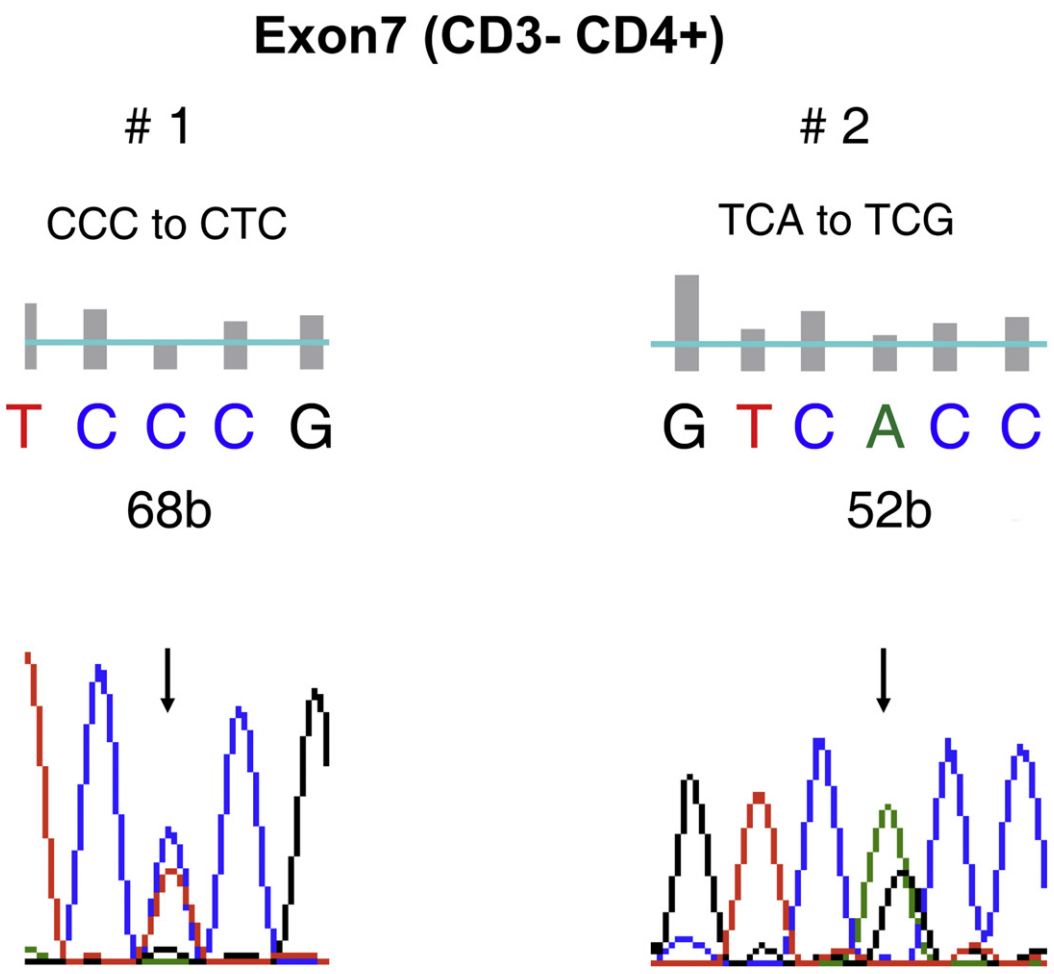

Fig. 4. *p53* sequence analysis in $CD3^{-}CD4^{+}$ cells in $p53^{+/-}$ mice at 56 weeks of age after 3 Gy whole-body irradiation at 8 weeks of age. Two mice showed heteromutation in *p53* intron 7. The point mutations were at 68 bases and at 52 bases before the beginning of *p53* exon 7.

non-irradiated $p53^{+/-}$ mice, one of nine mice showed *p53* allele loss (Fig. 2H).

Time course of p53 methylation frequency in $CD3^{+}CD4^{+}$ cells in $p53^{+/+}$ and $p53^{+/-}$ mice after3 Gy whole-body irradiation at 8 weeks of age

In non-irradiated $p53^{+/+}$ mice and $p53^{+/-}$ mice, *p53* methylation was detected in approximately 30% of mice in all experimental periods except for the non-irradiated control $p53^{+/+}$ mice at 8 weeks of age (Fig. 3). In irradiated $p53^{+/+}$ mice, *p53* methylation at 72 weeks of age occurred in eight of the 13 (62%) mice, which was increased compared to occurrence in three of the eight (38%) mice at 40 weeks of age. In irradiated $p53^{+/-}$ mice at 24 and 56 weeks of age, *p53* methylation occurred in five of the eight (63%) mice and in three of the five (60%) mice, respectively.

Sequence analysis

The DNA of the $p53^{+/+}$ mice and $p53^{+/-}$ mice were subjected to sequence analysis of exons 4 to 9 of the *p53* gene, but no mutations were detected except in two $p53^{+/-}$ mice. Mutations in *p53* intron 7 were found in those two irradiated $p53^{+/-}$ mice at 56 weeks of age. In Mouse 1, a point mutation was 68 bases before the beginning of *p53* exon 7 (a C to A heterozygous transition, CCC to CTC, proline to leucine). In Mouse 2, the mutation was 52 bases before the beginning of *p53* exon 7 (an A to G heterozygous transition, TCA to TCG, serine to serine) (Fig. 4).

Time course of protein expression of p53 and phospho-p53 in the spleens of $p53^{+/+}$ and $p53^{+/-}$ mice after 3 Gy whole-body irradiation at 8 weeks of age

The expressions of p53 in the non-irradiated mice gradually increased with age (Fig. 5A). In $p53^{+/+}$ mice at 24 and 72 weeks of age, the expression of p53 in the irradiated mice significantly decreased compared to the non-irradiated mice.

Specifically, the expression of phospho-p53 in the old irradiated mice was dramatically suppressed compared to that in the non-irradiated old mice (Fig. 5B). These data were consistent with the percentage of apoptotic cells that we previously reported (13). The percentage of apoptotic cells in

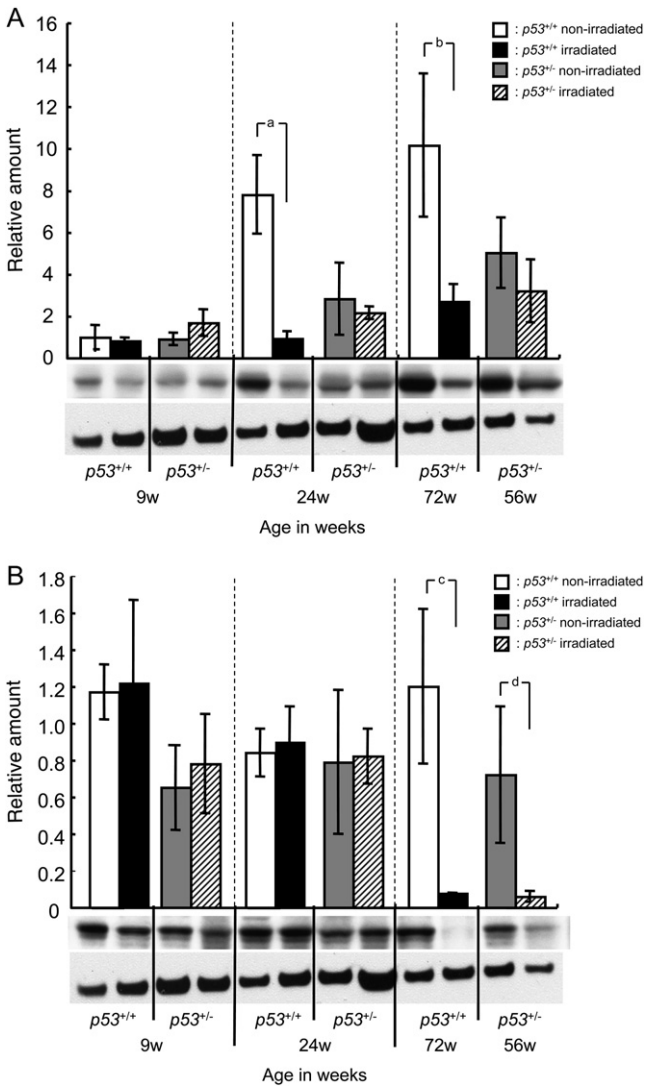

Fig. 5. Time course of protein expression of p53 and phospho-p53 (p53-ser15/18) in $p53^{+/+}$ and $p53^{+/-}$ mice after 3 Gy whole-body irradiation at 8 weeks of age. (A) p53. (B) phospho-p53. Western blot analysis was performed. Representative data are shown. The expression levels of p53 and phospho-p53 were normalized to actin. Each group contained 5 to 10 mice. Data are presented as means ± standard deviation. (A) $p < 0.0002$ compared to the control $p53^{+/+}$ mice at 24 weeks of age. (B) $p < 0.005$ compared to the control $p53^{+/+}$ mice at 72 weeks of age. (C) $p < 0.01$ compared to the control $p53^{+/+}$ mice at 72 weeks of age. (D) $p < 0.03$ compared to the control $p53^{+/-}$ mice at 56 weeks of age.

the irradiated old mice was decreased compared to that in the non-irradiated old mice.

DISCUSSION

Previously, we reported that irradiation at 8 weeks of age induces delayed TCR mutation in splenic T lymphocytes in $p53^{+/+}$ and $p53^{+/-}$ mice (13). The TCR mutation frequencies (MFs) increased to the maximum level 10 days after irradiation (at 9.4 weeks of age). The TCR MFs decreased to background levels at 16 weeks and 20 weeks of age in $p53^{+/+}$ and $p53^{+/-}$ mice, respectively. These continued at the same level until 60 weeks of age and 40 weeks of age in $p53^{+/+}$ mice and $p53^{+/-}$ mice, respectively. The delayed TCR MF in the irradiated mice increased significantly compared to that in the non-irradiated mice at 72 weeks of age and at 56 weeks of age in $p53^{+/+}$ mice and $p53^{+/-}$ mice, respectively.

In this study, the changes of the translocation frequency in chromosome 11 after irradiation were similar to that of the TCR MFs. We also found a delayed increase of translocation frequency in chromosomes 2 and 12 after irradiation at a young age (data not shown). These data suggest that irradiation at a young age induces delayed mutations. Furthermore, because the mouse *p53* locus is located on chromosome 11 (14), our data in this study suggest that the *p53* gene itself might be mutated. The *p53* gene is lost by a combination of deletion and/or mutation in 50% of all human tumors (19). Chromosome instability has been found in cancer cells (20). The genomic instability of *p53* might promote cancer development. However, there has been little or no clear evidence of chromosomal instability from atomic bomb survivors (21). The results of chromosomal instability are not always concordant in normal cells (22).

In the preliminary study, the *p53* allele loss was evaluated using DNA from spleen; however, there were no differences among any groups. In this study, we evaluated *p53* allele loss using DNA from $CD3^+CD4^+$ and $CD3^-CD4^+$ cells. The $CD3^+CD4^+$ cell is a mature T cell, and the $CD3^-CD4^+$ cell is a mutant T cell whose population is approximately 0.01% of total cells. Figure 2 shows that there were no differences in the *p53* allele loss in the $CD3^+CD4^+$ cells between irradiated mice and non-irradiated mice. It might be difficult to detect the *p53* allele loss in normal tissues or cells. Alternatively, in the $CD3^-CD4^+$ cells, the number of mice with *p53* allele loss increased among the irradiated mice. Usually, *p53* allele loss is found in tumor cells (23, 24). In the irradiated $p53^{+/-}$ mice, the *p53* allele loss was found at middle age, but it was not found in middle-aged $p53^{+/+}$ mice. The *p53* allele loss was found earlier in $p53^{+/-}$ mice than in $p53^{+/+}$ mice. Thus, genomic instability might be more easily induced in $p53^{+/-}$ mice.

It has been reported that *p53* methylation is increased in human carcinoma (25). To our knowledge, this is the first report that shows *p53* methylation in normal mouse tissues. As expected, *p53* methylation was increased earlier in $p53^{+/-}$ mice than in $p53^{+/+}$ mice. Epigenetic changes increase with aging and induce age-related diseases (*e.g.,* cancer and autoimmune diseases) (26). As liver tissue gradually worsens pathologically (normal–cirrhosis–carcinoma) *p53* methylation increases (25). Perhaps irradiation at a young age induces *p53* methylation and this relates to radiation-induced carcinogenesis.

We analyzed the DNA sequences in approximately 100 mice after irradiation at a young age. In this study, we detected the sequence mutation in only two $p53^{+/-}$ mice. Although only one base changed, the risk for disease is different. The arginine allele (CGC) in codon 72 of *p53* was shown to be a risk factor for invasive cervical cancer, whereas a proline allele (CCC) decreased the risk for cancer

(23). There might be a few events of sequence mutation in normal tissues, but this mutation may promote cancer or some diseases. In humans who had lupus, hypertrichosis, hemangioma, or cancer in the head-and-neck area, base changes in *p53* were found in skin dermatitis and/or carcinoma for 7 to 53 years after radiation treatment (27). In nickel sulfide–induced sarcoma (28) or in head-and-neck squamous cell carcinoma (23), transition or insertion in *p53* (including intron 7) was found and then p53 protein expression was suppressed (23). In this study, we showed a heterotransition in intron 7 at one allele. We suggest that these mutations may relate to suppress *p53* splicing and subsequently suppress p53 protein expression.

The p53 pathway is an important factor in cellular senescence (29). DNA damage and/or telomere dysfunction activate p53, and p53 induces senescence. In this study, we showed that the expression of p53 increased spontaneously with age in nonirradiated mice. Our data are consistent with these data. Alternatively, p53 expression and its function have been shown to decrease in elderly mice (30). In this study, the protein expression of p53 and phospho-p53 decreased in old irradiated mice compared to that in old nonirradiated mice. In the previous study, apoptotic activity decreased in old irradiated mice (13). These results support the idea that the lack of functional p53 results in an increased survival of cells with DNA damage and leads to an increased mutation frequency, either by a failure to block DNA replication that would have allowed time for DNA repair or by failed deletion of DNA-damaged cells in tissue by apoptosis. Loss of p53 function may be related to senescence. Jones *et al*. (31) have reported that ionizing radiation accelerates senescence in a p53-dependent manner in breast tumor cells. We suggest that irradiation at a young age might accelerate senescence.

In this study, we showed several kind of *p53* disorder (allele loss, methylation, and sequence transition) after irradiation at a young age. Our data suggest that irradiation at a young age induces these *p53* disorders with age. It is not clear whether these *p53* disorders happen dependently or independently of each other. In general, *p53* mutation induces senescence or tumorigenesis. Owing to a *p53* point mutation or loss of heterozygosity, the p53 expression and the apoptotic activity have been shown to be decreased in head-and-neck cancer (23). In one hypothesis regarding the progression of cancer (9, 32), in precancerous lesions, aberrant stimulation of cell proliferation leads to DNA replication stress that induces genomic instability. This genomic instability results from a *p53* disorder. In our opinion, these *p53* disorders after irradiation may relate to the genomic instability that induces various gene mutations. Because we showed that the delayed mutation after irradiation at a young age in $p53^{+/-}$ mice appeared earlier than that in $p53^{+/+}$ mice, it seems that the genomic instability causes senescence or tumorigenesis. We conclude that *p53* disorders might relate to suppress p53 protein expression after irradiation at a young age.

REFERENCES

1. Hall EJ. Radiation biology for pediatric radiologists. *Pediatr Radiol* 2009;39(Suppl 1):S57–S64.
2. Suzuki K, Takahara R, Kodama S, *et al*. In situ detection of chromosome bridge formation and delayed reproductive death in normal human embryonic cells surviving X irradiation. *Radiat Res* 1998;150:375–381.
3. Preston DL, Shimizu Y, Pierce DA, *et al*. Studies of mortality of atomic bomb survivors. Report 13: Solid cancer and noncancer disease mortality: 1950-1997. *Radiat Res* 2003; 160:381–407.
4. Pampfer S, Streffer C. Increased chromosome aberration levels in cells from mouse fetuses after zygote X-irradiation. *Int J Radiat Biol* 1989;55:85–92.
5. Holmberg K, Falt S, Johansson A, *et al*. Clonal chromosome aberrations and genomic instability in X-irradiated human T-lymphocyte cultures. *Mutat Res* 1993;286:321–330.
6. Wright EG, Coates PJ. Untargeted effects of ionizing radiation: Implications for radiation pathology. *Mutat Res* 2006;597:119–132.
7. Preston DL, Ron E, Tokuoka S, *et al*. Solid cancer incidence in atomic bomb survivors: 1958-1998. *Radiat Res* 2007;168:1–64.
8. Williams D. Radiation carcinogenesis: Lessons from Chernobyl. *Oncogene* 2008;27(Suppl 2):S9–S18.
9. Negrini S, Gorgoulis VG, Halazonetis TD. Genomic instability: An evolving hallmark of cancer. *Nat Rev Mol Cell Biol* 2010;11: 220–228.
10. Kim EH, Lee YJ, Bae S, *et al*. Heat shock factor 1-mediated aneuploidy requires a defective function of p53. *Cancer Res* 2009; 69:9404–9412.
11. MacLaren A, Slavin D, McGowan CH. Chk2 protects against radiation-induced genomic instability. *Radiat Res* 2009;172: 463–472.
12. MacPherson D, Kim J, Kim T, *et al*. Defective apoptosis and B-cell lymphomas in mice with p53 point mutation at Ser 23. *EMBO J* 2004;23:3689–3699.
13. Igari K, Igari Y, Okazaki R, *et al*. The delayed manifestation of T-cell receptor (TCR) variants in X-irradiated mice depends on Trp53 status. *Radiat Res* 2006;166:55–60.
14. Rotter V, Wolf D, Pravtcheva D, *et al*. Chromosomal assignment of the murine gene encoding the transformation-related protein p53. *Mol Cell Biol* 1984;4:383–385.
15. Gondo Y, Nakamura K, Nakao K, *et al*. Gene replacement of the p53 gene with the lacZ gene in mouse embryonic stem cells and mice by using two steps of homologous recombination. *Biochem Biophys Res Commun* 1994;202:830–837.
16. Michikawa Y, Sugahara K, Suga T, *et al*. In-gel multiple displacement amplification of long DNA fragments diluted to the single molecule level. *Anal Biochem* 2008;383:151–158.
17. Hulla JE, French JE, Dunnick JK. Chromosome 11 allelotypes reflect a mechanism of chemical carcinogenesis in heterozygous p53-deficient mice. *Carcinogenesis* 2001;22:89–98.
18. Okazaki R, Ootsuyama A, Norimura T. TP53 and TP53-related genes associated with protection from apoptosis in the radioadaptive response. *Radiat Res* 2007;167:51–57.
19. Hainaut P, Hollstein M. p53 and human cancer: the first ten thousand mutations. *Adv Cancer Res* 2000;77:81–137.
20. Kondo Y, Shen L, Ahmed S, *et al*. Downregulation of histone H3 lysine 9 methyltransferase G9a induces centrosome disruption and chromosome instability in cancer cells. *PLoS One* 2008;3. e2037.
21. Hamasaki K, Kusunoki Y, Nakashima E, *et al*. Clonally expanded T lymphocytes from atomic bomb survivors in vitro show no evidence of cytogenetic instability. *Radiat Res* 2009; 172:234–243.

22. Watson GE, Lorimore SA, Clutton SM, *et al*. Genetic factors influencing alpha-particle-induced chromosomal instability. *Int J Radiat Biol* 1997;71:497–503.
23. Schneider-Stock R, Mawrin C, Motsch C, *et al*. Retention of the arginine allele in codon 72 of the p53 gene correlates with poor apoptosis in head and neck cancer. *Am J Pathol* 2004;164: 1233–1241.
24. Tanooka H, Ootsuyama A, Sasaki H. Homologous recombination between p53 and its pseudogene in a radiation-induced mouse tumor. *Cancer Res* 1998;58:5649–5651.
25. Zhang C, Guo X, Jiang G, *et al*. CpG island methylator phenotype association with upregulated telomerase activity in hepatocellular carcinoma. *Int J Cancer* 2008;123:998–1004.
26. Grolleau-Julius A, Ray D, Yung RL. The role of epigenetics in aging and autoimmunity. *Clin Rev Allergy Immunol* 2010;39:42–50.
27. Franchi A, Massi D, Gallo O, *et al*. Radiation-induced cutaneous carcinoma of the head and neck: Is there an early role for p53 mutations? *Clin Exp Dermatol* 2006;31:793–798.
28. Govindarajan B, Klafter R, Miller MS, *et al*. Reactive oxygen-induced carcinogenesis causes hypermethylation of p16(Ink4a) and activation of MAP kinase. *Mol Med* 2002;8:1–8.
29. Vousden KH, Lu X. Live or let die: The cell's response to p53. *Nat Rev Cancer* 2002;2:594–604.
30. Feng Z, Hu W, Teresky AK, *et al*. Declining p53 function in the aging process: A possible mechanism for the increased tumor incidence in older populations. *Proc Natl Acad Sci U S A* 2007;104:16633–16638.
31. Jones KR, Elmore LW, Jackson-Cook C, *et al*. p53-Dependent accelerated senescence induced by ionizing radiation in breast tumour cells. *Int J Radiat Biol* 2005;81:445–458.
32. Gorgoulis VG, Vassiliou LV, Karakaidos P, *et al*. Activation of the DNA damage checkpoint and genomic instability in human precancerous lesions. *Nature* 2005;434:907–913.